Aging and Disease
www.aginganddisease.org
Volume 14, Number 2; 309-318, April 2023
http://dx.doi.org/10.14336/AD.2022.0827

Short Comminication

Zn-dependent β-amyloid Aggregation and its Reversal by the Tetrapeptide HAEE

Vladimir A. Mitkevich[1], Evgeny P. Barykin[1], Svetlana Eremina[1], Bibhusita Pani[2], Olga Katkova-Zhukotskaya[1], Vladimir I. Polshakov[3], Alexei A. Adzhubei[4], Sergey A. Kozin[1], Alexander S. Mironov[1], Alexander A. Makarov[1], Evgeny Nudler[2,5*]

[1]Engelhardt Institute of Molecular Biology, Russian Academy of Sciences, Moscow, Russia. [2]Department of Biochemistry and Molecular Pharmacology, New York University Grossman School of Medicine, New York, USA. [3]Faculty of Fundamental Medicine, M.V. Lomonosov Moscow State University, Moscow, Russia. [4]Washington University School of Medicine and Health Sciences, Washington, DC, USA. [5]Howard Hughes Medical Institute, New York University Grossman School of Medicine, New York, USA.

[Received May 20, 2022; Revised August 23, 2022; Accepted August 27, 2022]

ABSTRACT: The pathogenesis of Alzheimer's disease (AD) is associated with the formation of cerebral amyloid plaques, the main components of which are the modified Aβ molecules as well as the metal ions. Aβ isomerized at Asp7 residue (isoD7-Aβ) is the most abundant isoform in amyloid plaques. We hypothesized that the pathogenic effect of isoD7-Aβ is due to the formation of zinc-dependent oligomers, and that this interaction can be disrupted by the rationally designed tetrapeptide (HAEE). Here, we utilized surface plasmon resonance, nuclear magnetic resonance, and molecular dynamics simulation to demonstrate Zn^{2+}-dependent oligomerization of isoD7-Aβ and the formation of a stable isoD7-Aβ:Zn^{2+}:HAEE complex incapable of forming oligomers. To demonstrate the physiological importance of zinc-dependent isoD7-Aβ oligomerization and the ability of HAEE to interfere with this process at the organismal level, we employed transgenic nematodes overexpressing human Aβ. We show that the presence of isoD7-Aβ in the medium triggers extensive amyloidosis that occurs in a Zn^{2+}-dependent manner, enhances paralysis, and shortens the animals' lifespan. Exogenous HAEE completely reverses these pathological effects of isoD7-Aβ. We conclude that the synergistic action of isoD7-Aβ and Zn^{2+} promotes Aβ aggregation and that the selected small molecules capable of interrupting this process, such as HAEE, can potentially serve as anti-amyloid therapeutics.

Key words: Alzheimer disease, Aβ-Peptides, Isoaspartatic acid, Zinc, *Caenorhabditis* elegans

The development of AD comprises a cascade of pathogenic processes in brain tissue. Some of the major elements of this cascade are the aggregation of beta-amyloid (Aβ) with the formation of neurotoxic oligomers, hyperphosphorylation of tau, and neuroinflammation [1]. As a result, the characteristic histopathological picture of AD exhibits extracellular amyloid plaques and intracellular tau tangles. In the sporadic form of AD, accounting for 95% of disease cases, the molecular triggers for the pathological cascade remain unknown. Evidently, these triggers are age-related and affect the Aβ metabolism. Post-translationally modified forms of Aβ, the most common of which, is isomerized Asp7 (isoD7-Aβ) [2-4], are the candidates for such triggers. Isomerization of Asp is a spontaneous modification that accumulates over time during proteostasis decline [2, 5, 6]. In contrast to intact Aβ, intravenously administered isoD7-Aβ sharply accelerates cerebral amyloidosis in

***Correspondence should be addressed to:** Dr. Evgeny Nudler, Department of Biochemistry and Molecular Pharmacology, New York University Grossman School of Medicine, New York, NY 10016, USA. Email: evgeny.nudler@nyumc.org.

transgenic mice overexpressing human Aβ, potentially acting as an amyloid seeding. Moreover, synthetic isoD7-Aβ, rather than intact Aβ, causes a significantly higher level of tau phosphorylation in cell culture [7]. These findings suggest the role of isoD7-Aβ as a molecular trigger for the pathogenic cascade of AD and a potential drug target. Indeed, it has been recently shown that targeting isoD7-Aβ with an antibody attenuates AD-like pathology in transgenic mice [8]. The pathological properties of isoD7-Aβ may be a result of its enhanced ability to form oligomers in the presence of zinc ions [9, 10]. Zn^{2+} promotes the accumulation of Aβ oligomers in synapses in a neuronal activity-dependent manner, and of all the divalent cations, it plays the most significant role in the formation of senile plaques [11, 12]. However, there is no experimental data implicating the interaction of Zn^{2+} and isoD7-Aβ in AD pathology.

In this study, we utilized the *C. elegans* model of Aβ amyloidosis to study the effect of isoD7-Aβ and zinc ions on animal pathophysiology and aging. We show that the concurrent administration of Zn^{2+} and isoD7-Aβ leads to a significant increase in amyloidosis accompanied by the shortening of animals' lifespan. We further demonstrate that the tetrapeptide, HAEE, previously designed to counter the receptor toxicity of Aβ *in vitro* [13] , can prevent zinc-induced oligomerization of isoD7-Aβ, negate the pro-amyloid effects of isoD7-Aβ:Zn^{2+} in live animals, and restore their lifespan. Our surface plasmon resonance (SPR), nuclear magnetic resonance (NMR), and molecular dynamics (MD) studies indicate that the molecular mechanism underlying the anti-amyloid effect of HAEE relies on its specific zinc-dependent and stable binding to Aβ and isoD7-Aβ. Together, these results elucidate the fundamental role of non-covalent complexes between the zinc ion and isoD7-Aβ in triggering the pathological aggregation of endogenous Aβ molecules and suggest that the compounds targeting such complexes have a therapeutic potential.

MATERIALS AND METHODS

Materials

All chemicals and solvents were of HPLC-grade or better and were obtained from Sigma-Aldrich (St. Louis, MO, USA). Synthetic peptides (purity > 98% checked by RP-HPLC) $Aβ_{16}$ (Ac-DAEFRHDSGYEVHHQK-NH_2), H6R-$Aβ_{1-16}$ (Ac-DAEFRRDSGYEVHHQK-NH_2), isoD7-$Aβ_{16}$ (Ac-DAEFRH[isoD]SGYEVHHQK-NH_2, where [isoD] - isoaspartate), $Aβ_{42}$ (DAEFRHDSGYEVHHQKLVFFAEDVGSNKGAIIGLMVGGVVIA), isoD7-$Aβ_{42}$ (DAEFRH[isoD]SGYEVHHQKLVFFAEDVGSNKGAIIGLMVGGVVIA), GGGGC-$Aβ_{42}$, GGGGC-isoD7-$Aβ_{42}$, and Ac-HAEE-NH_2 were purchased from Biopeptide Co., LLC (San Diego, CA, USA). Zinc chloride (99.99%, ACROS Organics) was dried out for 1-2 hours at 150°C prior to weighing.

SPR analysis

All SPR measurements were carried out at 25°C using an optical biosensor Biacore 8K (GE Healthcare, USA) with CM4 optical chip. Covalent immobilization of the peptide ligands on the surface of the optical chip was performed using the sulfhydryl group of the C-terminal tetraglycylcysteine tag. Briefly, carboxyl groups on the chip surface were activated by serial injections of mixture of 0.4 M EDC/0.1 M NHS at a flow rate of 10 µL/min for 2 min and a solution of 80 mM PDEA in 100 mM borate buffer (pH 8.5) for 4 min. Solutions of 2 µM peptides in the immobilization buffer (10 mM acetate buffer, pH 4.5) were injected for 2 min at a flow rate of 10 µL/min (three repeats). Unreacted activated groups on the chip were blocked by further injection of a solution containing 50 mM cysteine, 1 M NaCl, 0.1 M sodium acetate (pH 4.3) for 4 min at a flow rate of 5 µL/min. Possible nonspecific analyte binding to the chip surface was evaluated using a free (control) channel of the biosensor exposed to the same treatments as the working channel except peptides. SPR signals were recorded in real time in resonance units (RU; 1 RU corresponds to 1 pg of analyte) and were presented in the form of sensorgrams showing time-dependent signal changes. A series of sensorgrams representing the difference of SPR-signals from working and control channels were obtained by serial injections of analyte solutions (Fig. 1B) through the working and control channels at a flow rate of 30 µL/min for 3 min. All SPR measurements were repeated 3 times. After each measurement the optical chip surface was regenerated by injecting an HBS-EP (0.01 M HEPES pH 7.4, 0.15 M NaCl, 3 mM EDTA, 0.005% v/v Surfactant P20) buffer for 30 s. Analyte samples were prepared in the running buffer (10 mM HEPES, pH 6.8 in the absence of Zn^{2+} and 10 mM HEPES, 100 µM $ZnCl_2$, pH 6.8). The obtained sensorgrams were analyzed with BIAevaluation v.4.1 software.

NMR experiments

Peptides $Aβ_{16}$, H6R-$Aβ_{16}$ and isoD7-$Aβ_{16}$ at the concentration of 0.2 – 8mM were dissolved in 10-20 mM bis-Tris-d_{19} (2,2-Bis(hydroxymethyl)-2,2′,2″-nitrilotriethanol-d_{19} with 98% ^2D enrichment) buffer solution (pH 6.8). Sodium salt of 3-(trimethylsilyl) propionic-2,2,3,3-d_4 acid (DSS) at a concentration of 10-20 µM was added as the standard. NMR spectra were measured at 278 K in 90% H_2O/10% D_2O with Bruker AVANCE 600 MHz spectrometer equipped with triple resonance (^1H, ^{13}C and

^{15}N) pulsed field z gradient probe. 1D NMR spectra were processed and analyzed using the Mnova software (Mestrelab Research, Spain). In order to monitor peptide-peptide interactions NMR titration experiments were carried out. Peptides at a concentration of 0.2-2.0 mM at pH 6.8 were titrated with a solution of HAEE and $ZnCl_2$ in a buffer of identical composition at the same pH value. 1D spectra were recorded for each titration point.

Modeling and MD simulations of the isoD7-Aβ:HAEE interactions

The templates for amyloid beta-peptide isoD7-$A\beta_{16}$ and HAEE structure modeling with zinc were taken from the PDB:2MGT solution NMR structure of zinc-induced dimer of the human amyloid beta-peptide metal binding domain 1-16 with Alzheimer's disease pathogenic English mutation H6R [9]. To obtain the isoD7-$A\beta_{16}$ structure, in one of the H6R-$A\beta_{1-16}$ molecules in the PDB:2MGT dimer, Asp7 was replaced with iso-asparagine and Arg6 was replaced with histidine, thus, $A\beta_{16}$ reverted to the iso-Asp7 primary structure. In the initial HAEE structure, hydrogens, acetyl, and amino (CH_3CO and NH_2 respectively) end groups were added and the resulting structure was minimized in water and relaxed for 100 ns using the Gromacs package [14]. HAEE was superposed with the structure of the second H6R-$A\beta_{16}$ molecule in the PDB:2MGT dimer, so that the positions of arginine and histidine atoms of $A\beta_{16}$ and HAEE, which coordinate zinc, corresponded as much as possible. This initial structure, after isoD7-$A\beta_{16}$ was replaced by isoD7-$A\beta_{42}$, was also used to model the isoD7-$A\beta_{42}$:HAEE interaction. The structure of isoD7-$A\beta_{42}$ was modeled by us previously [15]. Expert modeling was used to align the position of His13 side chain in isoD7-$A\beta_{42}$ with the corresponding side chain in the template zinc coordination interface. The resulting structures were solvated with TIP3P water and NaCl ions at a concentration of 115 mM. To model a zinc ion, two different special force fields based on quantum calculations were used, with practically no difference in the resulting Aβ:HAEE structures [16, 17]. The parametrization of the Aβ, HAEE, Glu, and His residues in coordinating zinc have been changed in accordance with the above force field. After 200 ps equilibration in NVT and NPT ensembles respectively the systems were simulated for 100 ns of MD production run at 300 K. All simulations were carried out using the particle mesh Ewald technique with repeating boundary conditions and 1 nm cut-offs, using the LINCS constraint algorithm with a 2 fs time step. The final structure after completion of MD simulation was taken as the representative structure. To analyze the stability of the Aβ final conformations, root mean square distance (RMSD) and root mean square fluctuation (RMSF) calculations of the MD trajectories were performed. The RMSD plot shows conformational stability of the structure during the MD simulation relevant to the reference structure.

Strains and growth conditions

C. elegans CL2120 (dvIs14 [(pCL12) unc-54::beta 1-42 +(pCL26) mtl-2::GFP]) and *C. elegans* CL2122 (dvIs15 [(pPD30.38) unc-54(vector) + (pCL26) mtl-2::GFP]) strains were obtained from the Caenorhabditis Genetics Center. The worms were handled according to standard methods without FUDR [18]. *E. coli* OP50 bacteria were grown overnight in Luria-Bertani broth and 50µl were spread atop NGM or NGMZn plates. NGMZn has 20µM $ZnSO_4$. Seeded plates were incubated at 30°C for ~16 hours and then for 1-2 hours at 15 or 25°C before worms were transferred. Lifespan and paralysis experiments (see below) were performed at 25°C for enhanced expression of Aβ. This temperature is standard when studying the effects of Aβ on *C. elegans* CL2120 strain [19].

Treatment with isoD7-Aβ$_{42}$ peptide and HAEE

Nematodes were purified from unwanted microflora by the alkaline hypochlorite method, grown to the L4 stage at 15°C on NGM plates with bacterial lawn. Approximately 140 animals were then placed in a drop of 0.2 ml M9-buffer +/- $ZnSO_4$ (20µM) +/- isoD7-$A\beta_{42}$ (40µM) +/- HAEE (4mM) and cultured for 4 hours at 25°C by stirring. Further, all contents were transferred to Petri plates with NGM or NGMZn with OP50 and placed in a temperature-controlled incubator at 25°C. Next day, worms were transferred onto similar media with a bacterial substrate and the lifespan was determined at 25°C (Supplementary Tables 3, 4).

Imaging and quantitative analysis of amyloid deposits

Nematodes were grown on NGM or NGMZn medium with a *E. coli* OP50 strain at 25°C and treated with amyloid peptides and/or HAEE as described above. At the A1 stage, the animals were stained with 1 mM X-34 (Sigma-Aldrich, St. Louis, MO, USA) in 10 mM Tris pH 8.0 for two hours. For de-staining, they were afterwards cultured for 16 hours on NGM or NGMZn with a bacterial lawn at the same temperature. Stained individual worms were mounted on glass slides in agar and anesthetized by incubation in 0.1% Na_3N. Amyloid aggregates were visualized with Leica TCS SP5 confocal microscope (Leica Microsystems GmbH, Wetzlar, Germany) using 405 nm laser for excitation and a 430-570 bandpass emission filter with 63x oil immersion objective. Worms were imaged as z-stacks of 10-15 images 4.1 µm thickness each. For imaging, standard Las X software (Leica

Microsystems GmbH, Wetzlar, Germany) with a plugin for confocal imaging was used. Acquired z-stacks were processed with Las X software to obtain maximum projections. Background subtraction and thresholding were performed by WCIF ImageJ with identical parameters for all images. Total plaque area, mean fluorescence intensity and plaques count were quantified for each worm in an area spanning from anterior end to posterior bulb. Data for plaque area is presented on graphs as individual values normalized by the amyloid load in control with bars representing sample means. The comparison of data groups was performed with ordinary one-way ANOVA. Post-hoc analysis was performed with the Tukey test. The Shapiro-Wilk test was used to confirm the normality of the dataset. Statistical analysis was performed with GraphPad Prism 9.1 software (GraphPad Software Inc., CA, USA). The representative nematode images for Fig. 2A were selected to have the plaques area that is close to the mean of each sample.

Paralysis assay

Synchronized eggs of CL2120 were grown to the L4 stage at 15°C on NGM plates with bacterial lawn, were treated with $ZnSO_4$, $A\beta_{42}$ (40 μM), isoD7-$A\beta_{42}$ (40μM), HAEE (4mM) and isoD7-$A\beta_{42}$ with HAEE at 25°C. Then, nematodes were transferred to Petri plates with NGM or NGMZn and OP-50, placed in a temperature-controlled incubator at 25°C. On the next day, worms were transferred onto similar media with a bacterial substrate and paralyzed nematodes were counted at equal time intervals. The worms that only moved their head or did not show a full-body movement when gently touched with a platinum loop were scored as paralyzed. For the paralysis experiments, we chose the days where we could clearly distinguish between paralysis and mortality. This conformed to the third and fourth days of their adult life. While at least three repeated trials were conducted, each experiment was performed using at least 100 worms. Details regarding repeated experiments and amounts of animals used for experiments are summarized in Supplementary Table 2. Mean fraction of paralyzed worms was compared between groups with two-way ANOVA, accounting for age and treatment. Post-hoc analysis was performed with the Tukey test. Statistical analysis was performed with GraphPad Prism 9.1 software.

Lifespan analysis

Lifespans were monitored at 25°C as described previously [20, 21]. All experiments were repeated at least three times and ≈130 worms were used for each experiment. Details regarding repeated experiments and amounts of animals used for experiments are summarized in Supplementary Tables 3, 4. In all cases, stage L4 worms were used at t = 0 for lifespan analyses and worms were transferred every other day to new agar plates. Worms were judged as dead when they ceased pharyngeal pumping and did not respond to prodding with a platinum wire. Escaped animals or animals with internal hatching were not included in lifespan calculation. Data was analyzed and Boltzmann sigmoid survival curves generated using the SciDAVis statistical analysis software package. Mean lifespans were compared in Microsoft Excel using the Student t test, applying one-tailed distribution and two-sample equal variance [22]. All lifespan plots represent the composites of all independent experiments tabulated in Supplementary Tables 3, 4. Mean percentage change ±SD of lifespan after treatment, relative to untreated control are indicated in each graph in the same color as the curve.

Statistical analysis

The applied statistical tests and software for each type of data are specified in the respective Methods subsections. For all of the data, before applying parametric statistical tests, the D'Agostino & Pearson normality test in GraphPad Prism 9.1 software was used to demonstrate that all sample data is distributed normally.

RESULTS

HAEE stably interacts with Aβ and interferes with its Zn^{2+}-dependent dimerization

In contrast to normal Aβ, both the full-length isomerized Aβ, isoD7-$A\beta_{42}$, and its metal-binding fragment, isoD7-$A\beta_{16}$, stimulate amyloidosis in transgenic mice [23, 24]. This correlates with the increased capacity of isoD7-$A\beta_{42}$ and isoD7-$A\beta_{16}$ for zinc-dependent aggregation [9]. We hypothesized that the contribution of isoD7-Aβ to the development of AD is based on the formation of zinc-bound complexes that promote pathological aggregation of Aβ (Fig. 1A). To test this hypothesis, we utilized a tool compound – the tetrapeptide HAEE, which was rationally designed to interact with the zinc-binding site of Aβ (^{11}EVHH^{14}) [13, 25].

We first used SPR analysis to study the interaction between the immobilized $A\beta_{42}$ or isoD7-$A\beta_{42}$ and the soluble HAEE tetrapeptide. In the absence of Zn^{2+}, no interaction of HAEE with immobilized amyloid peptides was detected (Supplementary Fig. 1). In the presence of 100 μM $ZnCl_2$, the sensorgrams of the HAEE interaction with both $A\beta_{42}$ or isoD7-$A\beta_{42}$ were obtained (Fig. 1B) and the interaction parameters calculated (Supplementary

Table 1). The K_D values for HAEE-Aβ$_{42}$ and HAEE-isoD7-Aβ$_{42}$ complexes were estimated to be 4.1±0.3 μM and 10.4±0.4 μM, respectively.

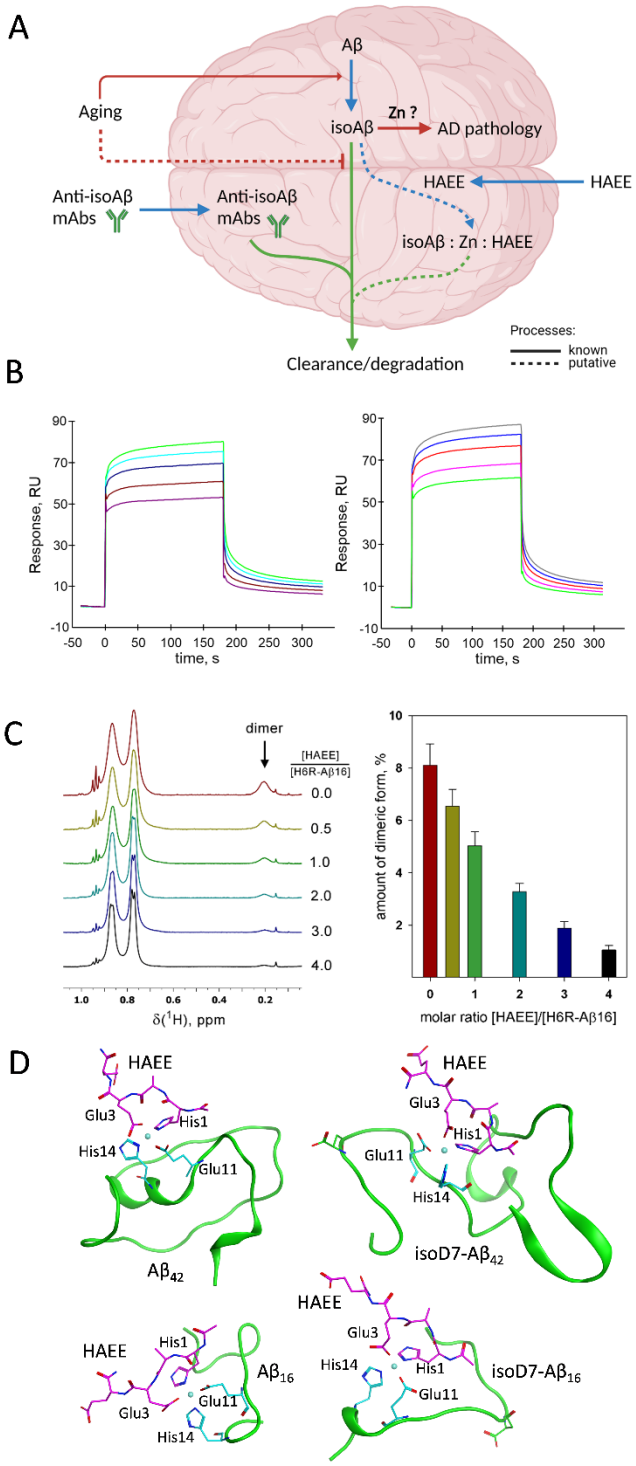

Figure 1. Interaction of HAEE with beta-amyloid. (A) A model for the contribution of isoD7-Aβ to AD pathology, and the possible ways of preventing its deleterious effects. Aβ spontaneously converts into isoD7-Aβ, which is accumulated over age, likely due to reduced Aβ clearance. Isomerized Aβ promotes AD pathology, potentially via formation of Zn-bound complexes serving as the seeds for a generation of neurotoxic oligomers. Treatment with anti-isoAβ antibodies is a promising therapeutic strategy already showing effectiveness in AD model mice [9]. HAEE was shown to hamper amyloid accumulation in animal models of AD [17], and its effect may be due to the formation of harmless isoAβ:Zn^{2+}:HAEE complexes, which are subject to degradation. **(B)** A set of sensorgrams illustrating paired interactions of various concentrations of HAEE (150, 300, 500, 1000, 1500 μM) with immobilized Aβ$_{42}$ (left panel) and isoD7-Aβ$_{42}$ (right panel) in the presence of 100 μM $ZnCl_2$, pH 6.8. **(C)** The addition of HAEE leads to a decrease in the amount of dimeric H6R-Aβ$_{16}$. Left panel: fragments of ^{1}H NMR spectra of a solution of the H6R-Aβ$_{16}$ peptide at a concentration of 1.6 mM, pH 6.8 in the presence of the 0.5 equivalent of $ZnCl_2$ during titration by HAEE. Right panel: a decrease in the content of dimeric H6R-Aβ$_{16}$ upon addition of HAEE. The amount of dimeric form is determined by the intensity of its characteristic signal at 0.2 ppm. **(D)** Interaction interface between HAEE (magenta) and Aβ$_{42}$, Aβ$_{16}$ (green) via zinc (left) and between HAEE (magenta) and isoD7-Aβ$_{42}$, isoD7-Aβ$_{16}$ (green) via zinc (right). Representative structures after 100-200 ns of MD simulation. Zinc is coordinated by oxygen atoms of glutamic acid and nitrogen atoms of histidine rings. ^{11}EVHH^{14} atoms are colored in cyan.

Next, we used NMR spectroscopy to obtain structural information on the interaction of HAEE with Aβ and isoD7-Aβ. Full-size Aβ quickly aggregates in solution in the presence of Zn^{2+} [26]. Therefore, we used a metal-binding fragment of Aβ (1-16 aa), which is an established model to study the role of Zn^{2+} in Aβ interactions . In the presence of Zn^{2+} the HAEE-induced chemical shift of $Aβ_{16}$ (Supplementary Fig. 2) and isoD7-$Aβ_{16}$ (Supplementary Fig. 3) signal was clearly observed. The presence of the tetrapeptide eliminated the signal at 0.2 ppm, which is characteristic of the dimeric form of the Aβ metal binding domain [9]. Thus, we conclude that HAEE inhibits the process of zinc-dependent dimerization in both $Aβ_{16}$ and isoD7-$Aβ_{16}$.

It should also be noted that the addition of Zn^{2+} to isoD7-$Aβ_{16}$ leads to its almost complete oligomerization and precipitation [9], as evident in the disappearance of the corresponding NMR signal (Supplementary Fig. 3) However, in the presence of HAEE, Zn^{2+} did not diminish the isoD7-$Aβ_{16}$ signal (Supplementary Fig. 3), highlighting the protective role of HAEE against its oligomerization.

It has been shown that an $Aβ_{1-16}$ variant with the so-called English (H6R) mutation (H6R-$Aβ_{16}$) exists as a mixture of monomeric and dimeric forms in the presence of Zn^{2+} [9]. The dimeric form has a well-resolved characteristic signal of the V12 methyl group at 0.2 ppm, which allows for a quantitative assessment of the dimeric state. The addition of HAEE to H6R-$Aβ_{16}$ in the presence of Zn^{2+} leads to a disappearance of the dimeric form (Fig. 1C, Supplementary Fig. 4). Of note, the affinity of Zn^{2+} to HAEE is almost an order of magnitude less than for H6R-$Aβ_{16}$ (Supplementary Fig. 5). Thus, the anti-dimerization effect of HAEE must be achieved via disrupting the H6R-$Aβ_{16}$ dimerization interface, not by competing for zinc.

Next, we utilized molecular dynamics (MD) to model Zn^{2+}-dependent interactions between HAEE and Aβ or its isoD7 isoform. MD simulations for 200 ns show the formation of stable complexes of $Aβ_{16}$:HAEE, isoD7-$Aβ_{16}$:HAEE, $Aβ_{42}$:HAEE and isoD7-$Aβ_{42}$:HAEE via the ^{11}EVHH^{14} site coordinated by Zn^{2+} (Fig. 1D). In contrast, only transient interactions can be seen without Zn^{2+} (Supplementary Fig. 6). We performed MD modelling for a number of systems with protonated and neutral histidines in $Aβ_{1-16}$ and HAEE and observed repeating multiple short-term interactions between HAEE and the ^{11}EVHH^{14} site of $Aβ_{16}$. In the isoD7-$Aβ_{16}$:Zn^{2+}:HAEE complex, the side chain interactions between Aβ Glu11/His14 and HAEE Glu3/His1 are coordinated by Zn^{2+} (Fig. 1D). In the case of isoD7-$Aβ_{42}$, a similar complex was formed (Fig. 1D). Moreover, the C-terminus of isoD7-$Aβ_{42}$ formed a loop, creating a cavity where Zn^{2+} interacted with HAEE. Additionally, four hydrogen bonds were formed between HAEE and His13, Asn27, Lys28 and Ala30 of isoD7-$Aβ_{42}$. This structural feature contributed to the stability of the isoD7-$Aβ_{42}$:Zn^{2+}:HAEE complex.

To assess the stability of the isoD7-$Aβ_{16}$:Zn^{2+}:HAEE and isoD7-$Aβ_{42}$:Zn^{2+}:HAEE complexes, the RMSD values were calculated as a graph showing the divergence of a structure in every MD trajectory frame from the final structure (Supplementary Fig. 7). The final structures of complexes remained stable. As the isoD7-$Aβ_{42}$:Zn^{2+}:HAEE structure features 4 additional intramolecular hydrogen bonds, it less flexible than the isoD7-$Aβ_{16}$:Zn^{2+}:HAEE structure (Supplementary Fig. 8).

Our previous experimental studies [9] and MD modeling [27] showed that in zinc-induced aggregation of Aβ, the residues coordinating zinc in the ^{11}EVHH^{14} site play a pivotal role. In this study, we show that the HAEE tetrapeptide efficiently binds these residues forming stable complexes, therefore these residues cannot participate in other interactions. Thus, we assume that the presence of HAEE tetrapeptide may prevent the aggregation of Aβ into unstructured conglomerates.

Exogenous HAEE prevents isoD7-$Aβ_{42}$:Zn^{2+}-mediated accelerated amyloidosis in the C. elegans model of AD

To study the therapeutic potential of HAEE in mitigating isoD7-$Aβ_{42}$:Zn^{2+}-mediated pathology *in vivo*, we adopted an improved *C. elegans* model of $Aβ_{42}$ toxicity (CL2120) that has been extensively used for AD research and drug screenings [28-32]. As the time required for a spontaneous isomerization of Asp7 in Aβ exceeds the lifespan of nematodes, it is highly unlikely that endogenous isoD7-Aβ would occur in CL2120 animals. Exogenous peptides, including Aβ-derived peptides, were previously shown to penetrate into *C. elegans* tissues upon addition to the growth or incubation medium [33-35], giving us an opportunity to study the effects of exogenous isoD7-Aβ and zinc ions on intrinsic $Aβ_{42}$ pathology.

CL2120 and transgenic control (CL2122) nematodes were treated with $Aβ_{42}$ or isoD7-$Aβ_{42}$, with and without Zn^{2+}, and amyloid aggregates visualized in live worms using amyloid-specific X-34 dye (Fig. 2A, Supplementary Fig. 9) [36]. In accordance with the previous data [28, 37], we observed age-dependent accumulation of $Aβ_{42}$ in the muscle tissue of CL2120 nematodes, but not in the CL2122 control (Supplementary Fig. 9). In worms exposed to the isoD7-$Aβ_{42}$/Zn^{2+} mixture, the area covered with plaques increased by 78% (Fig. 2A and B). Remarkably, the isoD7-$Aβ_{42}$/Zn^{2+} - induced amyloidosis was completely negated in the presence of HAEE peptide, as both the number of plaques and plaque area reduced back to the untreated group values (Fig. 2A and B). Notably, animals treated with isoD7-$Aβ_{42}$ in the absence of zinc, or with $Aβ_{42}$, with or without Zn^{2+}, did not show

any increase in the amyloid load (Fig. 2B, Supplementary Fig. 10).

Thus, exogenous isoD7-Aβ$_{42}$, not Aβ$_{42}$, is capable of promoting Aβ$_{42}$ amyloidosis in live animals in a Zn-dependent manner, whereas HAEE abrogates this pathological process.

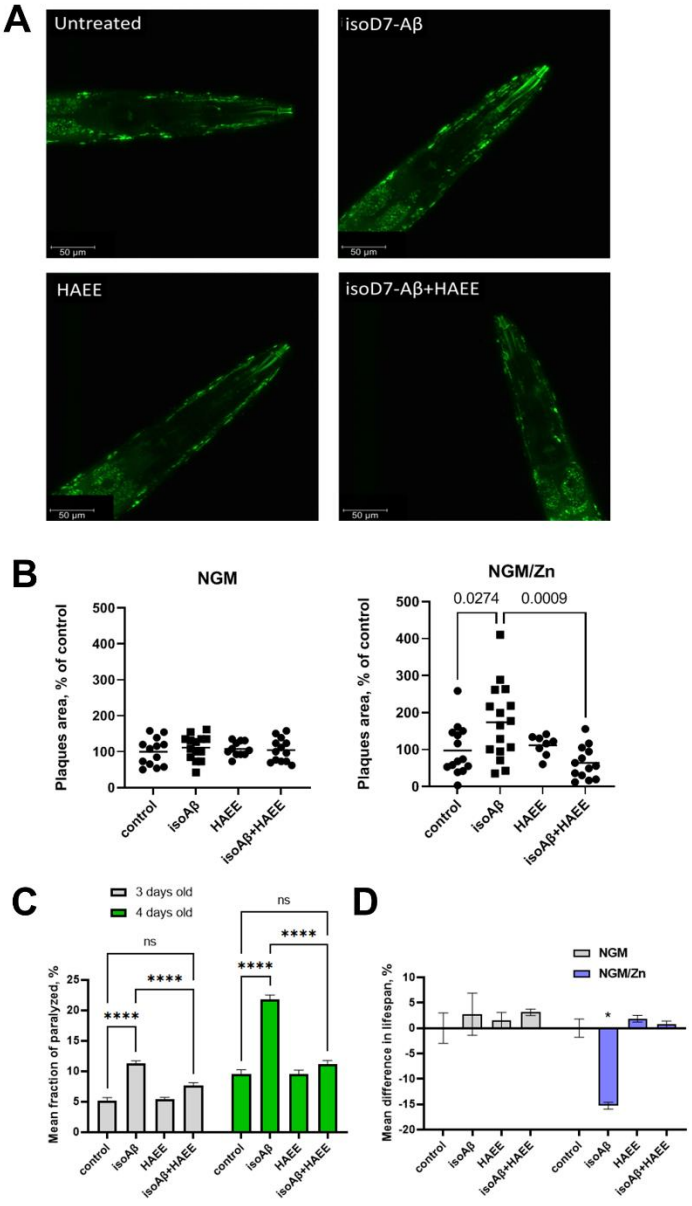

Figure 2. The effect of isoD7-Aβ$_{42}$ and HAEE in the presence of Zn^{2+} on amyloid load in *C. elegans*. **(A)** A visualization of amyloid aggregates in a *C. elegans* CL2120 strain untreated or incubated with isoD7-Aβ$_{42}$, HAEE, or isoD7-Aβ$_{42}$ and HAEE combined. Amyloid aggregates were stained with fluorescent dye X-34 in live animals. Shown are the maximum projections of z-stack images acquired with a confocal microscope. **(B)** The area covered with amyloid aggregates ("plaques") as a percentage of head area, detected by X-34 fluorescence. Worms were treated with 40 μM of isoD7-Aβ$_{42}$ (isoAβ), 4 mM of HAEE, these two peptides combined (isoAβ+HAEE) or received no treatment (control). After the incubation with peptides on NGMZn, the animals were stained with X-34 and amyloid aggregates were visualized with a confocal microscope. Data shown as individual values with a bar at sample mean. N for control, isoAβ, HAEE, isoAβ+HAEE treated worms equals 13, 15, 11, 13 for NGM group and 14, 16, 8, 12 for NGM/Zn group, respectively. Brackets represent statistically significant comparisons according to ANOVA with post-hoc Tukey test. P-values are indicated above the brackets. **(C)** The effects of isoD7-Aβ$_{42}$ and HAEE on the prevalence of a paralysis phenotype in *C. elegans* CL2120 of 3 days old (grey) and 4 days old (green). Treatment: 0.2 ml M9 buffer + $ZnSO_4$ (20μM) +/- isoD7-Aβ$_{42}$ (40 μM) +/- HAEE (4 mM). Strains were grown on NGMZn. Data is shown as the mean of 3 independent experiments ± SD. Brackets represent statistically significant comparisons according to ANOVA with post-hoc Tukey test. **** - $p<0.0001$, ns – non-significant. **(D)** The effects of isoD7-Aβ$_{42}$ and HAEE on *C. elegans* CL2120 lifespan. Left graph: Strains were grown on NGM. Treatment: 0.2 ml M9 buffer +/- isoD7-Aβ$_{42}$ (40 μM) +/- HAEE (4 mM). Right graph: Strains were grown on NGMZn. Treatment: 0.2 ml M9 buffer + $ZnSO_4$ (20μM) +/- isoD7-Aβ$_{42}$ (40μM) +/- HAEE (4 mM). Data is shown as the mean difference in lifespan ± SD (%) of treated worms compared to control. The results of 3 independent experiments are presented. * - $p<0.0001$, according to Student t test.

HAEE prevents isoD7-Aβ$_{42}$:Zn^{2+}-induced paralysis and decelerates aging in AD model animals

The deposition of amyloid aggregates reflects the increased concentration of toxic amyloid oligomers, which can be deleterious to surrounding tissue. In CL2120 nematodes Aβ$_{42}$ is expressed in body wall muscle cells, resulting in severe age progressive-paralysis [28]. Therefore, we studied if the isoD7-Aβ$_{42}$/Zn^{2+} mixture affects the paralysis of nematodes. We found that isoD7-Aβ$_{42}$/Zn^{2+} accelerates paralysis in CL2120 animals, whereas HAEE suppresses this effect (Fig. 2C). The effect was not observed for Aβ$_{42}$/Zn^{2+} nor amyloid peptides in the absence of Zn^{2+} (Supplementary Fig. 11, Supplementary Table 2).

Next, we studied how the lifespan of nematodes is affected by exogenous amyloid peptides and zinc. CL2120 and CL2122 animals have similar lifespans at 20°C [38]. The addition of Aβ$_{42}$, with or without zinc ions,

to NGM did not affect the mean lifespan of CL2120 or CL2122 animals (Supplementary Fig. 12, Supplementary Table 3). In contrast, the addition of the isoD7-Aβ_{42} peptide to Zn^{2+}-containing media significantly decreased the lifespan of CL2120 animals, not control CL2122 animals (Fig. 2D, Supplementary Fig. 12, Supplementary Table 4). Without Zn^{2+}, the negative effect of exogenous isoD7-Aβ_{42} on the Aβ_{42} transgenic animals was not detected.

Nematodes accumulate zinc in response to high zinc diet, and dietary zinc can be toxic to *C. elegans* [39, 40]. Taking into account the higher affinity of isoAsp7-containing peptide to zinc [10], it could promote toxicity by increasing the zinc uptake in a chelated form. However, the incubation medium contained only 20 μM of zinc, which is two orders of magnitude below the IC50 [39], thus arguing that the toxicity is due to isoD7-Aβ itself.

Strikingly, the addition of HAEE completely restored the shortened lifespan of isoD7-Aβ_{42} + Zn^{2+} - treated CL2120 animals. HAEE itself has no effect on the lifespan of CL2120 or CL2122 animals (Supplementary Fig. 13, Supplementary Table 4). Thus, we conclude that systemic amyloidosis promoted by exogenous isoD7-Aβ_{42} in the Zn-dependent manner shortens the animals' lifespan, which can be cured by a rationally designed anti-isoD7-Aβ_{42} tetrapeptide (HAEE).

DISCUSSION

Alzheimer's disease has a multifactorial pathology [41-45]. One of the main neuromorphological signs of AD is dense and diffused extracellular aggregates of Aβ – the amyloid plaques in brain tissue [1]. Accruing evidence suggests that the pathological cascade of AD is triggered by the accumulation of soluble neurotoxic Aβ oligomers [46]. In addition to the well-known effect of zinc ions on Aβ aggregation [11, 12], the formation of neurotoxic oligomers can be stimulated by the post-translational modifications of Aβ, such as Asp7 isomerization [8].

To identify the fundamental role of non-covalent complexes between Zn^{2+} and isoD7-Aβ in triggering pathological aggregation of endogenous Aβ molecules, we used the HAEE tetrapeptide as a specific molecular tool capable of binding Aβ and disrupting its metal-dependent dimerization interface. The formation of stable complexes of beta-amyloid peptides (^{11}EVHH^{14} region) with HAEE, in the presence of Zn^{2+}, is shown using SPR (Fig. 1B, Supplementary Table 1). Based on the structure of the zinc-bound H6R-Aβ_{16} dimer [9], models of the isoD7-Aβ complex with HAEE and Zn^{2+} for the full-length peptide and its metal-binding domain were created (Fig. 1D). Other potential Zn^{2+}-interacting sites are predicted to further stabilize the complex via strong electrostatic forces, consistent with the results of the 200 ns MD run (Supplementary Fig. 7). NMR studies further show that HAEE shifts the equilibrium between monomeric and dimeric Aβ towards its monomeric form in the presence of zinc ions (Fig. 1C), indicating that it disrupts dimerization of Aβ via blocking the primary zinc-recognition site at ^{11}EVHH^{14}.

The *in vivo* data validates our mechanistic model of Zn^{2+}-mediated amyloidosis. Strikingly, the amyloid burden in nematodes treated with isoD7-Aβ increased almost two-fold if zinc was present in the NGM medium (Fig. 2). The simultaneous presence of zinc ions and isoD7-Aβ in the diet also resulted in a significant enhancement in animal paralysis and shortening of the lifespan. If either zinc was absent from the medium or non-modified Aβ_{42} was used for the treatment, the changes in the amyloid load, paralysis, and lifespan were not detected.

It has been previously shown that, unlike Aβ_{42}, exogenous isoD7-Aβ_{42} stimulates amyloidosis in transgenic mice, but the role of zinc in this process remained unknown. The present results imply that soluble Aβ species form zinc-bound complexes that enter *C. elegans* tissue. In the case of isoD7-Aβ_{42}, such complexes promote amyloidosis and toxicity leading to animal paralysis and lifespan reduction. In the presence of HAEE, the combination of Zn^{2+} and isoD7-Aβ fails to induce amyloidosis and associated pathologies in *C. elegans* (Fig. 2), which demonstrates that oligomeric isoAβ:Zn assemblies trigger the morbific effect. Notably, the HAEE peptide did not affect the endogenous amyloidosis in untreated transgenic *C. elegans*.

Taken together, the experiments with *C. elegans* demonstrate, for the first time, the importance of both zinc ions and the isomerization of Asp7 for systemic toxic aggregation of native Aβ. They also identify HAEE as a small molecular agent capable of blocking this pathological process at the organismal level, suggesting a novel anti-amyloid therapeutic approach.

Acknowledgments

We thank Sergei Zhokhov for assistance in measurements of NMR spectra, Yuri Mezentsev for assistance in SPR experiments and Anna Tolstova for help in bioinformatics. This work was supported by the Blavatnik Family Foundation, Howard Hughes Medical Institute (E.N.), and the Russian Science Foundation grant No. 19-74-30007 (A.A.M.).

Competing interests

The authors declare no competing interests.

Author Contributions

VAM, AAM and EN conceptualized this study. VAM, EPB, BP and EN designed the experiments. EPB, SE, BP, and OK performed all C. elegans experiments. VIP performed NMR experiments and analysis. AAA performed modelling and MD simulations. SAK performed SPR experiments. VAM, EPB, SE, BP, and EN analyzed data. VAM, AAM and EN wrote the paper with input from all co-authors.

Data and materials availability

The data that support the findings of this study are either included in the Manuscript and Supplementary information or available from the corresponding author upon reasonable request.

Supplementary Materials

The Supplementary data can be found online at: www.aginganddisease.org/EN/10.14336/AD.2022.0827.

References

[1] Walsh DM, Selkoe DJ (2020). Amyloid β-protein and beyond: the path forward in Alzheimer's disease. Curr Opin Neurobiol, 61:116-124.

[2] Barykin EP, Mitkevich VA, Kozin SA, Makarov AA (2017). Amyloid β modification: a key to the sporadic Alzheimer's disease? Frontiers in Genetics, 8:58.

[3] Kozin SA, Mitkevich VA, Makarov AA (2016). Amyloid-b containing isoaspartate 7 as potential biomarker and drug target in Alzheimer's disease. Mendeleev Communications, 26:269-275

[4] Mukherjee S, Perez KA, Lago LC, Klatt S, McLean CA, Birchall IE, et al. (2021). Quantification of N-terminal amyloid-β isoforms reveals isomers are the most abundant form of the amyloid-β peptide in sporadic Alzheimer's disease. Brain Commun, 3:fcab028.

[5] Clarke S (2003). Aging as war between chemical and biochemical processes: protein methylation and the recognition of age-damaged proteins for repair. Ageing Res Rev, 2:263-285.

[6] Shimizu T, Matsuoka Y, Shirasawa T (2005). Biological significance of isoaspartate and its repair system. Biol Pharm Bull, 28:1590-1596.

[7] Zatsepina OG, Kechko OI, Mitkevich VA, Kozin SA, Yurinskaya MM, Vinokurov MG, et al. (2018). Amyloid-β with isomerized Asp7 cytotoxicity is coupled to protein phosphorylation. Sci Rep, 8:3518.

[8] Gnoth K, Piechotta A, Kleinschmidt M, Konrath S, Schenk M, Taudte N, et al. (2020). Targeting isoaspartate-modified Aβ rescues behavioral deficits in transgenic mice with Alzheimer's disease-like pathology. Alzheimers Res Ther, 12:149.

[9] Istrate AN, Kozin SA, Zhokhov SS, Mantsyzov AB, Kechko OI, Pastore A, et al. (2016). Interplay of histidine residues of the Alzheimer's disease Ab peptide governs its Zn-induced oligomerization. Scientific Reports, 6:21734.

[10] Tsvetkov PO, Popov IA, Nikolaev EN, Archakov AI, Makarov AA, Kozin SA (2008). Isomerization of the Asp7 residue results in zinc-induced oligomerization of Alzheimer's disease amyloid beta(1-16) peptide. Chembiochem, 9:1564-1567.

[11] Kepp KP (2012). Bioinorganic chemistry of Alzheimer's disease. Chem Rev, 112:5193-5239.

[12] Lee JY, Cole TB, Palmiter RD, Suh SW, Koh JY (2002). Contribution by synaptic zinc to the gender-disparate plaque formation in human Swedish mutant APP transgenic mice. Proc Natl Acad Sci U S A, 99:7705-7710.

[13] Barykin EP, Garifulina AI, Tolstova AP, Anashkina AA, Adzhubei AA, Mezentsev YV, et al. (2020). Tetrapeptide Ac-HAEE-NH(2) Protects α4β2 nAChR from Inhibition by Aβ. Int J Mol Sci, 21:6272.

[14] Abraham MJ, Murtola T, Schulz R, Páll S, Smith JC, Hess B, et al. (2015). GROMACS: High performance molecular simulations through multi-level parallelism from laptops to supercomputers. SoftwareX, 1-2:19-25.

[15] Barykin EP, Garifulina AI, Kruykova EV, Spirova EN, Anashkina AA, Adzhubei AA, et al. (2019). Isomerization of Asp7 in Beta-Amyloid Enhances Inhibition of the alpha7 Nicotinic Receptor and Promotes Neurotoxicity. Cells, 8.

[16] Del Frate G, Nikitin A (2018). Including Electronic Screening in Classical Force Field of Zinc Ion for Biomolecular Simulations. ChemistrySelect, 3:12367-12370.

[17] Macchiagodena M, Pagliai M, Andreini C, Rosato A, Procacci P (2020). Upgraded AMBER Force Field for Zinc-Binding Residues and Ligands for Predicting Structural Properties and Binding Affinities in Zinc-Proteins. ACS Omega, 5:15301-15310.

[18] Brenner S (1974). The genetics of Caenorhabditis elegans. Genetics, 77:71-94.

[19] Lu X, Zhang Y, Li H, Jin Y, Zhao L, Wang X (2021). Nicotine prevents in vivo Aβ toxicity in Caenorhabditis elegans via SKN-1. Neurosci Lett, 761:136114.

[20] Apfeld J, Kenyon C (1999). Regulation of lifespan by sensory perception in Caenorhabditis elegans. Nature, 402:804-809.

[21] Dillin A, Crawford DK, Kenyon C (2002). Timing requirements for insulin/IGF-1 signaling in C. elegans. Science, 298:830-834.

[22] Gusarov I, Gautier L, Smolentseva O, Shamovsky I, Eremina S, Mironov A, et al. (2013). Bacterial nitric oxide extends the lifespan of C. elegans. Cell, 152:818-830.

[23] Kozin SA, Cheglakov IB, Ovsepyan AA, Telegin GB, Tsvetkov PO, Lisitsa AV, et al. (2013). Peripherally Applied Synthetic Peptide isoAsp7-Aβ(1-42) Triggers

Cerebral β-Amyloidosis. Neurotoxicity Research, 24:370-376.

[24] Kulikova AA, Cheglakov IB, Kukharsky MS, Ovchinnikov RK, Kozin SA, Makarov AA (2016). Intracerebral injection of metal-binding domain of Aβ comprising the isomerized Asp7 increases the amyloid burden in transgenic mice. Neurotoxicity Research, 29:551-557.

[25] Zolotarev YA, Mitkevich VA, Shram SI, Adzhubei AA, Tolstova AP, Talibov OB, et al. (2021). Pharmacokinetics and Molecular Modeling Indicate nAChRα4-Derived Peptide HAEE Goes through the Blood-Brain Barrier. Biomolecules, 11:909.

[26] Bush AI, Pettingell WH, Multhaup G, d Paradis M, Vonsattel JP, Gusella JF, et al. (1994). Rapid induction of Alzheimer A beta amyloid formation by zinc. Science, 265:1464-1467.

[27] Tolstova AP, Makarov AA, Adzhubei AA (2021). Zinc Induced Aβ16 Aggregation Modeled by Molecular Dynamics. International Journal of Molecular Sciences, 22:12161.

[28] McColl G, Roberts BR, Pukala TL, Kenche VB, Roberts CM, Link CD, et al. (2012). Utility of an improved model of amyloid-beta ($A\beta_{1-42}$) toxicity in Caenorhabditis elegans for drug screening for Alzheimer's disease. Mol Neurodegener, 7:57.

[29] Ewald CY, Li C (2010). Understanding the molecular basis of Alzheimer's disease using a Caenorhabditis elegans model system. Brain Struct Funct, 214:263-283.

[30] Alexander AG, Marfil V, Li C (2014). Use of Caenorhabditis elegans as a model to study Alzheimer's disease and other neurodegenerative diseases. Front Genet, 5:279.

[31] Chen X, Barclay JW, Burgoyne RD, Morgan A (2015). Using C. elegans to discover therapeutic compounds for ageing-associated neurodegenerative diseases. Chem Cent J, 9:65.

[32] Dostal V, Link CD (2010). Assaying β-amyloid toxicity using a transgenic C. elegans model. J Vis Exp, 44:2252.

[33] Diomede L, Romeo M, Cagnotto A, Rossi A, Beeg M, Stravalaci M, et al. (2016). The new β amyloid-derived peptide Aβ1-6A2V-TAT(D) prevents Aβ oligomer formation and protects transgenic C. elegans from Aβ toxicity. Neurobiol Dis, 88:75-84.

[34] Romeo M, Stravalaci M, Beeg M, Rossi A, Fiordaliso F, Corbelli A, et al. (2017). Humanin Specifically Interacts with Amyloid-β Oligomers and Counteracts Their in vivo Toxicity. J Alzheimers Dis, 57:857-871.

[35] Xu J, Yuan Y, Zhang R, Song Y, Sui T, Wang J, et al. (2019). A deuterohemin peptide protects a transgenic Caenorhabditis elegans model of Alzheimer's disease by inhibiting Aβ(1-42) aggregation. Bioorg Chem, 82:332-339.

[36] Link CD, Johnson CJ, Fonte V, Paupard M, Hall DH, Styren S, et al. (2001). Visualization of fibrillar amyloid deposits in living, transgenic Caenorhabditis elegans animals using the sensitive amyloid dye, X-34. Neurobiol Aging, 22:217-226.

[37] Fay DS, Fluet A, Johnson CJ, Link CD (1998). In vivo aggregation of beta-amyloid peptide variants. J Neurochem, 71:1616-1625.

[38] Minniti AN, Rebolledo DL, Grez PM, Fadic R, Aldunate R, Volitakis I, et al. (2009). Intracellular amyloid formation in muscle cells of Abeta-transgenic Caenorhabditis elegans: determinants and physiological role in copper detoxification. Mol Neurodegener, 4:2.

[39] Davis DE, Roh HC, Deshmukh K, Bruinsma JJ, Schneider DL, Guthrie J, et al. (2009). The cation diffusion facilitator gene cdf-2 mediates zinc metabolism in Caenorhabditis elegans. Genetics, 182:1015-1033.

[40] Roh HC, Collier S, Guthrie J, Robertson JD, Kornfeld K (2012). Lysosome-related organelles in intestinal cells are a zinc storage site in C. elegans. Cell Metab, 15:88-99.

[41] Bourdenx M, Dovero S, Thiolat ML, Bezard E, Dehay B (2017). Lack of spontaneous age-related brain pathology in Octodon degus: a reappraisal of the model. Sci Rep, 7:45831.

[42] De Strooper B, Simons M, Multhaup G, Van Leuven F, Beyreuther K, Dotti CG (1995). Production of intracellular amyloid-containing fragments in hippocampal neurons expressing human amyloid precursor protein and protection against amyloidogenesis by subtle amino acid substitutions in the rodent sequence. Embo j, 14:4932-4938.

[43] Edrey YH, Medina DX, Gaczynska M, Osmulski PA, Oddo S, Caccamo A, et al. (2013). Amyloid beta and the longest-lived rodent: the naked mole-rat as a model for natural protection from Alzheimer's disease. Neurobiol Aging, 34:2352-2360.

[44] Shivers BD, Hilbich C, Multhaup G, Salbaum M, Beyreuther K, Seeburg PH (1988). Alzheimer's disease amyloidogenic glycoprotein: expression pattern in rat brain suggests a role in cell contact. Embo j, 7:1365-1370.

[45] Steffen J, Krohn M, Paarmann K, Schwitlick C, Brüning T, Marreiros R, et al. (2016). Revisiting rodent models: Octodon degus as Alzheimer's disease model? Acta Neuropathol Commun, 4:91.

[46] Mattson MP (2004). Pathways towards and away from Alzheimer's disease. Nature, 430:631-639.